NASA-TM-111946

THE SCHWINGER VARIATIONAL METHOD

Winifred M. Huo

NASA Ames Research Center, Moffett Field, CA 94035, U.S.A.

1. INTRODUCTION

Variational methods have proven to be invaluable tools in theoretical physics and chemistry, both for bound state problems and for the study of collision phenomena. For collisional problems variational methods can be grouped into two types, those based on the Schrödinger equation and those based on the Lippmann-Schwinger equation. The Hulthén-Kohn[1-3] method belongs to the first type, and their modern development for electron-molecule scattering, incorporating complex boundary conditions, is reported in chapter 1 of this book by Rescigno et al.[4] An offshoot of the Hulthén-Kohn variational method is the variational R-matrix method.[5,6] In chapter 8 of this book Schneider[7] presents a general discussion of the R-matrix method, including the variational R-matrix.

The Schwinger variational (SV) method, which Schwinger introduced in his lectures at Harvard University and subsequently published in 1947,[8] belongs to the second category. The application of the SV method to e-molecule collisions and molecular photoionization has been reviewed previously.[9-12] The present chapter discusses the implementation of the SV method as applied to e-molecule collisions. Since this is not a review of cross section data, cross sections are presented only to serve as illustrative examples.

In the SV method, the correct boundary condition is automatically incorporated through the use of the Green's function. Thus SV calculations can employ basis functions with arbitrary boundary condition. This feature enables the use of an L^2 basis for scattering calculations, and provided the initial motivation for applying the SV method to atomic and molecular physics.[10,13] The initial success led to the development of the iterative Schwinger method[14] which uses single-center expansion techniques and also an iterative procedure to improve the initial basis set. The iterative Schwinger method has been used extensively to study molecular photoionization.[15] For e-molecule collisions, it is used at the static-exchange level to study elastic scattering[16] and coupled with the distorted wave approximation to study electronically inelastic scattering.[17]

The Schwinger multichannel (SMC) method, originally formulated by Takatsuka and McKoy,[18,19] is the first modern computational method for e-molecule collisions explicitly designed to treat the multicenter nature of a polyatomic target. When Gaussian

Computational Methods for Electron-Molecule Collisions
Edited by W.M. Huo and F.A. Gianturco, Plenum Press, New York, 1995

functions are used for the L^2 basis and plane waves for the incoming electron, all two-electron repulsion integrals are calculated analytically. It is also a multichannel method and readily treats electronic inelastic scattering as well as polarization effects in elastic scattering. In addition, integrals involving the Green's function, generally considered the bottleneck in the SV method, can now be computed efficiently and accurately using the insertion method.[20] Alternatively, highly parallel computing can be effectively employed in the numerical integration over the final three-dimensions for this type of integrals.[12] The SMC method has been found to be robust, and has been employed to study molecules of various sizes and with different bonding types. For example, it has been used to study the electronic excitation of [1,1,1] propellane by electron impact,[21] the largest polyatomic molecule studied so far by *ab initio* methods. It has also been used to study electron scattering from the ground state of BeCO, a molecule with a weak van der Waals bond, to simulate scattering from an adsorbate in a physisorbed system.[22] Since the SMC method is the most commonly used SV treatment for e-molecule scattering, the main topic of this chapter will deal with its implementation.

Both the SMC and iterative Schwinger methods calculate fixed-nuclei, body-frame T-matrices. Domcke[23] has demonstrated that nuclear dynamics in e-molecule collisions can be treated efficiently using projection operator formalism and Green's function approach. Results of the fixed-nuclei SMC calculation can be coupled directly with Domcke's treatment of nuclear dynamics. As an example, we present a calculation of vibrational excitations of N_2 by electron impact which combines these two treatments.

2. THE LIPPMANN-SCHWINGER EQUATION AND THE SCHWINGER VARIATIONAL PRINCIPLE

In the integral equation approach, we look for solutions of the Lippmann-Schwinger (LS) equation instead of the Schrödinger equation. Let the Hamiltonian of the electron + molecule system be written as

$$H = \sum_{i=1}^{N+1} \left(-\frac{1}{2}\nabla_i^2 - \sum_{k=1}^{N_p} \frac{Z_k}{|\mathbf{r}_i - \mathbf{R}_k|} + \sum_{j>i}^{N+1} \frac{1}{r_{ij}} \right) + \sum_{k=1}^{N_p} \left(-\frac{1}{2m_k}\nabla_k^2 + \sum_{l>k}^{N_p} \frac{Z_k Z_l}{R_{kl}} \right). \quad (1)$$

Here i,j and k,l sum over electrons and nuclei, respectively; Z_k and m_k denote the charge and mass of the kth nucleus. Also, atomic units will be used unless specified otherwise. Note that H is symmetric and its eigenfunction antisymmetric with respect to electron exchange. Rewriting H as

$$H = H_o + V, \quad (2)$$

with

$$H_o = H_M - \frac{1}{2}\nabla_{N+1}^2, \quad (3)$$

and

$$V = \sum_{i=1}^{N} \frac{1}{|\mathbf{r}_{N+1} - \mathbf{r}_i|} - \sum_{k=1}^{N_p} \frac{Z_k}{|\mathbf{r}_{N+1} - \mathbf{R}_k|}. \quad (4)$$

The use of $N+1$ to label the continuum electron is completely arbitrary. Also, H_M is the molecular Hamiltonian with eigenfunctions Φ_m,

$$H_M \Phi_m = \mathcal{E}_m \Phi_m. \quad (5)$$

The LS equation is given by,

$$\Psi^{(+)} = S + G^{(+)} V \Psi^{(+)}. \tag{6}$$

with

$$\lim_{\delta \to 0} (E - H_o + i\delta) G^{(+)}(E') = \delta(E - E'). \tag{7}$$

and S is the solution of the corresponding homogeneous equation.[1/] Here we use the boundary condition of an incoming plane wave and outgoing spherical waves, which has been incorporated into the Green's function $G^{(+)}$. Due to this feature, it is not necessary to use trial functions which satisfy the correct boundary conditions in solving the LS equation. The Green's function $G^{(+)}$ is expressed in terms of the molecular eigenfunctions and the interaction-free Green's function.

$$G^{(+)}(E) = -\frac{1}{2\pi} \sum_{m=1} |\Phi_m\rangle \frac{exp(ik_m|\mathbf{r}_{N+1} - \mathbf{r}_{N+1}'|)}{|\mathbf{r}_{N+1} - \mathbf{r}_{N+1}'|} \langle \Phi_m|. \tag{8}$$

where

$$\frac{1}{2} k_m^2 + \mathcal{E}_m = E, \tag{9}$$

The summation m is over the entire molecular spectrum, including continuum states. When $\mathcal{E}_m > E$, k_m becomes imaginary, corresponding to a bound electron. Indeed, including the continuum spectrum of the target allows the outgoing electron to be different from the incoming electron, a necessary feature in order to account for electron exchange.[2/]

Based on the LS equation for $\Psi^{(+)}$, and the corresponding equation for $\Psi^{(-)}$ with outgoing plane wave and incoming spherical waves boundary conditions,

$$\Psi^{(-)} = S + G^{(-)} V \Psi^{(-)}.$$

the Transition matrix, or T-matrix, of a scattering process can be written as

$$T_{mn} = \langle S_m|V|\Psi_n^{(+)}\rangle = \langle \Psi_m^{(-)}|V|S_n\rangle = \langle \Psi_m^{(-)}|V - VG^{(+)}V|\Psi_n^{(+)}\rangle. \tag{10}$$

It is readily seen that a combination of the above expressions

$$T_{mn} = \langle S_m|V|\Psi_n^{(+)}\rangle + \langle \Psi_m^{(-)}|V|S_n\rangle - \langle \Psi_m^{(-)}|V - VG^{(+)}V|\Psi_n^{(+)}\rangle. \tag{11}$$

results in a T-matrix that is stationary with respect to first-order variations in $\Psi^{(+)}$ and $\Psi^{(-)}$, respectively.

$$\delta T_{mn} = \langle S_m|V|\Psi_n^{(+)} + \delta\Psi_n^{(+)}\rangle + \langle \Psi_m^{(-)}|V|S_n\rangle - \langle \Psi_m^{(-)}|V - VG^{(+)}V|\Psi_n^{(+)} + \delta\Psi_n^{(+)}\rangle - T_{mn}$$

$$= 0,$$

[1/] We choose to use a homogeneous solution which is the product of the target wave function and the free-particle wave function of the continuum electron, without antisymmetrization between the two. As pointed out in Ref. 24, it is not necessary to antisymmetrize both the initial and final wave functions explicitly. If $\Psi^{(+)}$ is antisymmetric, then the T-matrix element will automatically pick up the antisymmetric part of S. This convention is used here so that the same S will also apply to the SMC equation discussed in Sec. 3.

[2/] A different approach to account for exchange is to incorporate the Hamiltonian with permuted indices into the interaction potential, $U = V + \sum_i P_{i,N+1}(H - E)$. See Bransden et al.[25]

and

$$\delta T_{mn} = \langle S_m|V|\Psi_n^{(+)}\rangle + \langle \Psi_m^{(-)} + \delta\Psi_m^{(-)}|V|S_n\rangle - \langle \Psi_m^{(-)} + \delta\Psi_m^{(-)}|V - VG^{(+)}V|\Psi_n^{(+)}\rangle - T_{mn}$$

$$= 0.$$

Equation (11) is referred to as the linear form of the Schwinger variational principle.

In most e-molecule calculations, it is common practice to expand $\Psi_n^{(+)}$ and $\Psi_m^{(-)}$ in terms of a set of antisymmetrized $N+1$-electron trial functions f,

$$\Psi_n^{(+)} = \sum_r b_r(\boldsymbol{k}_n) f_r, \tag{12}$$

and

$$\Psi_m^{(-)} = \sum_s c_s(\boldsymbol{k}_m) f_s. \tag{13}$$

Eq. (11) gives

$$T_{mn} = \sum_r b_r\langle S_m|V|f_r\rangle + \sum_s c_s\langle f_s|V|S_n\rangle - \sum_r\sum_s b_r c_s\langle f_s|V - VG^{(+)}V|f_r\rangle. \tag{14}$$

The requirement that T_{mn} be stationary with respect to first order variations in the expansion coefficients b_r and c_s,

$$\partial T_{mn}/\partial b_r = 0,$$

$$\partial T_{mn}/\partial c_s = 0,$$

gives the following relationships,

$$b_r = \sum_s D_{rs}\langle f_s|V|S_n\rangle, \tag{15}$$

$$c_s = \sum_r \langle S_m|V|f_r\rangle D_{rs}, \tag{16}$$

with

$$(D^{-1})_{rs} = \langle f_r|V - VG^{(+)}V|f_s\rangle. \tag{17}$$

The resulting variational stable expression for T_{mn} is[26]

$$T_{mn} = \sum_{rs}\langle S_m|V|f_r\rangle D_{rs}\langle f_s|V|S_n\rangle. \tag{18}$$

Equation (18) has the advantage that it is independent of the normalization of $\Psi_n^{(+)}$ and $\Psi_m^{(-)}$.

The advantages of the Schwinger variational method have been discussed previously.[9, 10] Because the correct boundary condition is already incorporated into the Green's function and because the variational stable expression of the T-matrix in Eq. (18) is independent of normalization, it allows flexibility in the choice of a basis. Furthermore, the wave function in Eqs. (11) and (18) always appears together with the potential, i.e., $V|\Psi_n^{(+)}\rangle$ or $\langle\Psi_m^{(-)}|V$. Thus a trial basis for $\Psi_n^{(+)}$ needs only to cover the region of space where V does not vanish. This feature allows us to use an L^2 basis to represent $\Psi_n^{(+)}$ when V is a short-range potential.

Another advantage of the SV method is that the Schwinger variational principle is one rank higher than the Kohn variational principle.[27, 28] If the same trial wave function is used, the Schwinger method should give a better converged result. It should be noted

that, in comparing the two methods, it is important to use the *same* trial basis because the Kohn method, which requires basis functions with the correct boundary condition, generally uses a trial basis different from the Schwinger method.

A major drawback of the SV method lies in the difficulty in calculating the Green's function matrix elements.[9] The matrix element $\langle \Psi_m^{(-)}|VG^{(+)}V|\Psi_n^{(+)}\rangle$ in Eq. (11) or $\langle f_r|VG^{(+)}V|f_s\rangle$ in Eq. (17) are nine-dimensional integrals if V includes a two-electron potential. This obstacle has recently been removed when it is demonstrated[20] that the insertion technique can be used with efficiency and good accuracy for the evaluation of these matrix elements. This will be discussed in Sec. 3.5. Alternatively, highly parallel computing can be employed for the 3-dimension numerical integration over the wave vector in these matrix elements.

2.1. A Simple Example of Potential Scattering

To illustrate the use of Eq. (18) and to demonstrate the convergence property of the SV method, consider the elastic scattering of an s-wave by a weak potential U. The initial state is described by the Riccati-Bessel function,

$$S = j_0(kr).$$

Since the potential is weak, $j_0(kr)$ can also be used as a reasonable representation for the trial functions of Ψ^+ and $\Psi^{(-)}$. Here the trial functions are of the form

$$\Psi^{(+)} = b_0 j_0(kr),$$

$$\Psi^{(-)} = c_0 j_0(kr).$$

Because the initial boundary condition is described by S in the LS equation, the coefficients b_0 and c_0 need not be set to 1. Instead, they are used as variational parameters and optimized. Note that the use of $j_0(kr)$ as a trial basis is an example of a basis which does not satisfy the correct boundary condition. Otherwise a combination of Riccati-Bessel and Neumann functions should be employed. Because $\Psi^{(+)}$ and $\Psi^{(-)}$ are expanded in a one term expansion, the inverse of the D-matrix, in Eq. (17), is just the inverse of the matrix element itself. From Eq. (18), the SV expression of the elastic T-matrix is given by

$$T_{00} = \frac{\langle j_0(kr)|U|j_0(kr)\rangle\langle j_0(kr)|U|j_0(kr)\rangle}{\langle j_0(kr)|U - UG^{(+)}U|j_0(kr)\rangle}.$$

Since U is a weak potential, we can write

$$\frac{1}{\langle j_0(kr)|U - UG^{(+)}U|j_0(kr)\rangle} = \frac{1}{\langle j_0(kr)|U|j_0(kr)\rangle}\left(1 + \frac{\langle j_0(kr)|UG^{(+)}U|j_0(kr)\rangle}{\langle j_0(kr)|U|j_0(kr)\rangle} + \ldots\right).$$

Substituting the above into the expression for T_{00}, we find

$$T_{00} = \langle j_0(kr)|U|j_0(kr)\rangle + \langle j_0(kr)|UG^{(+)}U|j_0(kr)\rangle + \ldots$$

The first and second terms of T_{00} correspond to the first and second Born terms, respectively.

In Eq. (10) three non-variational expressions for T_{00} are given. They give identical results if the exact $\Psi^{(+)}$ and $\Psi^{(-)}$ are used. Otherwise they give different values for the T-matrix. The first relation,

$$T_{00} = \langle S|U|\Psi^{(+)}\rangle,$$

gives the Born approximation for T_{00}.[3/]

$$T_{00} = \langle j_0(kr)|U|j_0(kr)\rangle.$$

This result is inferior to the SV expression. Using the third relation in Eq. (10),

$$T_{00} = \langle \Psi^{(-)}|U - UG^{(+)}U|\Psi^{(+)}\rangle,$$

T_{00} deviates even further from the variationally stable result,

$$T_{00} = \langle j_0(kr)|U|j_0(kr)\rangle - \langle j_0(kr)|UG^{(+)}U|j_0(kr)\rangle.$$

Now the second Born term is subtracted from, instead of added to, the first Born term. The above exercise clearly illustrates the power of the variational method.

3. THE SCHWINGER MULTICHANNEL METHOD (SMC)

Currently, the most frequently used form of the Schwinger variational principle for e-molecule collisions originates from the work of Takatsuka and McKoy.[18, 19] As seen below, while this formulation is based on the Schwinger variational principle, its equation of motion is obtained by combining the LS and Schrödinger equations. These equations are coupled via the introduction of a projection operator P which projects into the open-channel target space. In the following, we shall first consider some of the properties of Takatsuka's projection operator, then derive the SMC equation. Implementation of the method will then be delineated. Efficient evaluation of the Green's function matrix elements, generally considered a bottleneck in the Schwinger method, will be discussed and extension to include correlated target functions will also be presented.

3.1. The N-Electron Projection Operator P

The projection operator P introduced by Takatsuka and McKoy projects into the open channel target space. Hence it is an N-electron projection operator and different from the Feshbach projection operator,[29] which is a $N+1$-electron operator.

$$P = \sum_{m=1}^{M} |\Phi_m(1,2,\ldots,N)\rangle\langle\Phi_m(1,2,\ldots,N)|, \tag{19}$$

with m summing over all energetically accessible target states. P satisfies the idempotent property,

$$P^2 = P,$$

and commutes with H_o

$$PH_o = H_oP.$$

To illustrate the difference between P and P_{N+1}, the Feshbach projection operator, consider the simplest case when the target wave function Φ_i is expressible in terms of a closed shell, single determinental wave function,

$$\Phi_i(1,2,\ldots,N) = \mathcal{A}\left\{\phi_1\alpha(1)\phi_1\beta(2)\ldots\phi_{N/2}\alpha(N-1)\phi_{N/2}\beta(N)\right\}.$$

[3/] Here $\Psi^{(+)}$ is not optimized and $b_0 = 1$ is used.

Here α and β denote spin functions and $\mathcal{A}$ the antisymmetrizer. If the wave function of the continuum electron, $g_i(N+1)$, is orthogonal to all the target orbitals, then the $S_z = 1/2$ component of Ψ_i becomes

$$\Psi_i(1,2,\ldots,N,N+1) = \mathcal{A}\left\{\phi_1\alpha(1)\phi_1\beta(2)\ldots\phi_{N/2}\beta(N)g_i\alpha(N+1)\right\}.$$

We have

$$P\Psi_i(1,2,\ldots,N,N+1) = \frac{1}{\sqrt{N+1}}\Phi_i(1,2,\ldots,N)g_i\alpha(N+1), \tag{20}$$

and

$$\langle\Psi_j|HP|\Psi_i\rangle = \frac{1}{N+1}\langle\Psi_j|H|\Psi_i\rangle. \tag{21}$$

On the other hand, the Feshbach projection operator is defined in terms of the $N+1$-electron open channel functions,

$$P_{N+1} = \sum_m |\Psi_m(1,2,\ldots,N,N+1)\rangle\langle\Psi_m(1,2,\ldots,N,N+1)|.$$

where Ψ_m satisfies the correct asymptotic boundary condition. The function Ψ_i is an open channel function in the terminology of the Feshbach projector formalism if g_i satisfies the correct boundary condition. In that case,

$$P_{N+1}\Psi_i = \Psi_i. \tag{22}$$

A comparison of Eqs. (20) and (22) shows how the two projection operators differ. Also note that Takatsuka's projection operator treats Ψ_i as an open channel function as long as it is associated with an energetically accessible target function, regardless of the behavior of g_i at the boundary. The Feshbach projection operator, on the other hand, includes Ψ_i in the open channel space only if g_i has the correct boundary behavior.

It should be noted that Eq. (20) may not be applicable when the orthogonality constraint between the continuum electron function and the target function is relaxed, and/or when the target is described by more sophisticated wave functions. Consider the simple case of $X^1\Sigma_g^+ \rightarrow b^3\Sigma_u^+$ excitation of H_2 by electron impact. Let the wave function for the $X^1\Sigma_g^+$ state be represented by

$$\Phi_X = \mathcal{A}\{1\sigma_g\alpha(1)1\sigma_g\beta(2)\},$$

and the three spin components of the $b^3\Sigma_u^+$ state by

$$\Phi_{b,S_z=1} = \mathcal{A}\{1\sigma_g\alpha(1)1\sigma_u\alpha(2)\},$$

$$\Phi_{b,S_z=0} = \mathcal{A}\{1\sigma_g(1)1\sigma_u(2)\frac{1}{\sqrt{2}}[\alpha(1)\beta(2)+\beta(1)\alpha(2)]\},$$

$$\Phi_{b,S_z=-1} = \mathcal{A}\{1\sigma_g\beta(1)1\sigma_u\beta(2)\}.$$

It is well established that in calculating this transition, terms of the form

$$\Psi_a = \mathcal{A}\{1\sigma_g\alpha(1)1\sigma_u\alpha(2)1\sigma_u\beta(3)\}, \tag{23}$$

and

$$\Psi_b = \mathcal{A}\{1\sigma_g\alpha(1)1\sigma_g\beta(2)1\sigma_u\alpha(3)\}, \tag{24}$$

should be included in the expansion of the wave function. These are usually called 'penetration' or 'recorrelation terms' because they relax the enforced orthogonality between the continuum and target functions. Let the projection operator P be generated from the four target functions above. We then have

$$P\Psi_a = \frac{1}{\sqrt{3}}\Phi_{b,S_z=1}(1,2)1\sigma_u\beta(3) - \frac{1}{\sqrt{6}}\Phi_{b,S_z=0}(1,2)1\sigma_u\alpha(3). \tag{25}$$

This simple example illustrates how the operation of P depends on the type of functions used.

3.2. The SMC Equation

The projected LS equation is

$$P\Psi_n^{(+)} = S_n + G_P^{(+)}V\Psi_n^{(+)}, \tag{26}$$

The projected Green's function, $G_P^{(+)}$, is defined in the open channel space by,

$$G_P^{(+)} = -\frac{1}{2\pi}\sum_{m=1}^{M}|\Phi_m\rangle\frac{exp(ik_m|\boldsymbol{r}_{N+1} - \boldsymbol{r}_{N+1}{}'|)}{|\boldsymbol{r}_{N+1} - \boldsymbol{r}_{N+1}{}'|}\langle\Phi_m|.$$

Multiplying Eq. (26) from the left by V and rearranging, we find

$$(VP - VG_P^{(+)}V)\Psi_n^{(+)} = VS_n \tag{27}$$

Equation (27) describes only the open channel functions, whereas a complete description of $\Psi_n^{(+)}$ also requires the closed channel component. To do this, we use the following identity

$$aP + (1 - aP) = 1. \tag{28}$$

Note that in association with the operation of P, a parameter a, called the projection parameter, is introduced. It is seen from Eqs. (20) and (25) that the operation of P not only removes the antisymmetrization between the target function and continuum orbital, but also generates a constant which multiplies the resulting function. Thus the introduction of a is a logical step. The determination of a will be discussed after the SMC equation is derived.

The closed channel contribution is described by the projected Schrödinger equation,

$$(1 - aP)\hat{H}\Psi_n^{(+)} = 0, \tag{29}$$

with

$$\hat{H} = E - H,$$
$$\hat{H} = \hat{H}_o - V,$$

and

$$\hat{H}_o = E - H_o.$$

Note that

$$\begin{aligned} P\hat{H} &= P\hat{H}_o - PV \\ &= \frac{1}{2}(\hat{H}_oP + P\hat{H}_o) - PV \\ &= \frac{1}{2}(\hat{H}P + P\hat{H}) + \frac{1}{2}(VP - PV). \end{aligned}$$

Equation (29) can be rewritten as

$$[\hat{H} - \frac{a}{2}(\hat{H}P + P\hat{H}) + \frac{a}{2}(PV - VP)]\Psi_n^{(+)} = 0. \tag{30}$$

The SMC equation is obtained by dividing Eq. (30) by a and adding it to Eq. (27),

$$A^{(+)}\Psi_n^{(+)} = VS_n, \tag{31}$$

with $A^{(+)}$ the SMC operator,

$$A^{(+)} = \left\{\frac{1}{2}(PV + VP) - VG_P^{(+)}V + \frac{1}{a}\hat{H} - \frac{1}{2}(P\hat{H} + \hat{H}P)\right\}. \tag{32}$$

The SMC equation[4/] uses the LS equation to describe the open channel component of $\Psi^{(+)}$ and the Schrödinger equation for the closed channel component. Because it includes both the open and closed channel components, it provides a complete solution to the scattering problem.[30]

Using the SMC equation instead of the LS equation, the Schwinger variational expression for the T-matrix is

$$T_{mn} = \langle S_m|V|\Psi_n^{(+)}\rangle + \langle\Psi_m^{(-)}|V|S_n\rangle - \langle\Psi_m^{(-)}|A^{(+)}|\Psi_n^{(+)}\rangle. \tag{33}$$

If the scattering wave function is expressed in terms of $N + 1$-electron trial functions f, as in Eqs. (12) and (13), the variational stable expression for T_{mn} is the same as Eq. (18),

$$T_{mn} = \sum_{rs}\langle S_m|V|f_r\rangle D_{rs}\langle f_s|V|S_n\rangle. \tag{34}$$

but with

$$(D^{-1})_{rs} = \langle f_r|A^{(+)}|f_s\rangle. \tag{35}$$

3.3. The Projection Parameter a

The SMC equation is incomplete until a is chosen. A number of ways of determining a have been considered in the literature, and they are described below:

(a) Based on the hermiticity of the principal-value SMC operator. Takatsuka and McKoy[18, 19] and Lima and McKoy[30] argued that the variational stability of T_{mn} requires

$$A^{(+)\dagger} = A^{(-)}. \tag{36}$$

In other words, the principal-valued SMC operator A must be Hermitian. Otherwise, T_{mn} will be unstable with respect to first order variation of either $\delta\Psi_n^{(+)}$ or $\delta\Psi_m^{(-)}$. While Eq. (36) is readily satisfied for trial functions consisting only of L^2 functions, Takatsuka and McKoy noted that, if the trial functions included (shielded) spherical Bessel and Neumann (or Hankel) functions, Eq. (36) is not valid because the matrix element of the kinetic energy operator between Bessel and Neumann functions is non-Hermitian. In this case, they showed that if the projection parameter is chosen to be

$$a = N + 1, \tag{37}$$

4/ Takatsuka and McKoy's original derivation[18,19] used the principal-value SMC operator, A, obtained by replacing $G_P^{(+)}$ with the principal-value Green's function, G_P. Similarly, the wave functions are replaced by those with standing wave boundary conditions. However, most subsequent numerical calculations used $A^{(+)}$.

the following matrix element vanishes in the open channel space,

$$\langle P\Psi_m|\frac{1}{a}\hat{H} - \frac{1}{2}(P\hat{H} + \hat{H}P)|P\Psi_n\rangle = 0.$$

The operator $\frac{1}{a}\hat{H} - \frac{1}{2}(P\hat{H} + \hat{H}P)$ is the only part of the SMC operator which involves the kinetic energy operator. If its matrix element is identically zero in the open channel space, Eq. (36) is guaranteed to hold even for a basis which includes spherical Bessel and Neumann functions.

(b) Based on the stability of the T-matrix with respect to first order variation of a. Huo and Weatherford[31] pointed out that the SMC equation automatically incorporates the proper boundary condition through the Green's function. Thus it is unnecessary to include functions with the proper boundary condition in an SMC basis. Indeed, almost all SMC calculations carried out so far use an L^2 basis. In that case, Eq. (36) is satisfied independent of a. Even if continuum functions are included in the basis, the use of δ-function normalizable continuum functions would again ensure the validity of Eq. (36). (A Neumann function is not δ-function normalizable). Instead, they considered the role of a as a weight factor for the relative contribution between the open and closed channel space. Thus a should be treated as a variation parameter and its optimal choice should be based on the variational stability,

$$\partial T_{mn}/\partial a = 0.$$

If $\Psi_n^{(+)}$ and $\Psi_m^{(-)}$ are expanded in terms of Eqs. (12) and (13), the above condition results in the following expression,

$$\sum_r \sum_s b_r \langle f_r|\hat{H}|f_s\rangle c_s = 0. \tag{38}$$

Equation (38) is to be solved together with Eqs. (15) and (16) so that a can be determined simultaneously with the expansion coefficients b_r and c_s.

Using Eqs. (12) and (13), Eq. (38) can be rewritten as

$$\langle \Psi_n^{(+)}|\hat{H}|\Psi_m^{(-)}\rangle = 0.$$

Thus it will be automatically satisfied if $\Psi_n^{(+)}$ and/or $\Psi_m^{(-)}$ satisfy the Schrödinger equation,

$$\hat{H}\Psi_n^{(+)} = 0,$$

or

$$\hat{H}\Psi_m^{(-)} = 0.$$

Under these circumstances, T_{mn} will be stable for any finite value of a, including $a = N + 1$. This result is related to how the LS and Schrödinger equations are combined in the SMC equation. A true solution should satisfy both equations, with the result independent of how the SMC operator is partitioned. However, in practical calculations we search for a variationally stable T_{mn}. Equation (38), which is identical to the configuration-interaction (CI) equation in electronic structural calculations, is much more amenable to practical calculations than the Schrödinger equation itself. Generally we have found that an iterative solution of a, coupled with the calculation of T_{mn}, adds approximately 10% to the cost of an SMC calculation with fixed a.

(c) Based on supplementing the projected LS equation. An alternate proof for Eq. (37) was provided by Winstead and McKoy.[32] Instead of using the SMC equation, they looked for the variational stability of T_{mn} by using the projected LS equation, Eq. (26), alone.

$$T_{mn} = \langle S_m|V|\Psi_n^{(+)}\rangle + \langle \Psi_m^{(-)}|V|S_n\rangle - \langle \Psi_m^{(-)}|VP - VG_P^{(+)}V|\Psi_n^{(+)}\rangle.$$

While the above expression is not variationally stable, they found that stability can be achieved by adding to the projected LS equation a term $Q\hat{H}$.

$$T_{mn} = \langle S_m|V|\Psi_n^{(+)}\rangle + \langle \Psi_m^{(-)}|V|S_n\rangle - \langle \Psi_m^{(-)}|VP - VG_P^{(+)}V + Q\hat{H}|\Psi_n^{(+)}\rangle, \qquad (39)$$

with

$$Q = P - R.$$

The operator R, applied to an antisymmetrized $N + 1$-electron function, removes the antisymmetrization between an N-electron function and the one-electron function for the $(N + 1)$th electron. Thus we have

$$\langle \Psi_m^{(-)}|R\hat{H}|\Psi_n^{(+)}\rangle = \frac{1}{N+1}\langle \Psi_m^{(-)}|\hat{H}|\Psi_n^{(+)}\rangle.$$

It can be readily shown that Eq. (39) leads to a variational stable expression for T_{mn}, with Eq. (37) for a. However, unlike Eq. (28), the operators P and Q do not span the complete space. In view of the fact that P is an N-electron operator whereas R, and hence Q, is an $N + 1$-electron operator, we have

$$P + Q \neq 1.$$

In contrast with the result of Lima and McKoy[30] who used Eq. (28) to prove the completeness of the solutions of the SMC equation, the present approach fails to demonstrate that the solution of the operator equation

$$(VP - VG_P^{(+)}V + Q\hat{H})\Psi^{(+)} = S,$$

is complete.

3.4. Implementation of the SMC Method

The trial wave function $\Psi_n^{(+)}$ in the SMC method is expanded by

$$\Psi_n^{(+)} = \sum_{i=1}^{M}\sum_j b_{ij}^{(n)}\mathcal{A}\{\Phi_i(1\ldots N)\chi_j(N+1)\} + \sum_l b_l^{(n)}\Theta_l(1\ldots N+1), \qquad (40)$$

where the index i sums over open channel target functions, j sums over the one-electron basis set χ used to expand the continuum electron function, and l sums over Θ, the antisymmetrized $N + 1$-electron configuration-state-function (CSF). The expansion coefficients $b_{ij}^{(n)}$ and $b_l^{(n)}$ are to be determined variationally.

So far, all SMC calculations on molecules have used target functions represented by a Cartesian Gaussian basis. Also, they make use of the fact that the correct boundary conditions have been automatically incorporated in the SMC equation and employ an L^2 basis of Cartesian Gaussian functions to represent the continuum electron. Thus the trial form of $\Psi_n^{(+)}$ contains no information of its behavior at the boundary. Instead, its initial condition is given by S_n and the outgoing wave by $G_P^{(+)}V\Psi_n^{(+)}$ in the SMC

equation. For collisions with long range potentials, where an L^2 basis is inadequate, the higher partial wave contributions are determined using a Born closure approximation.[41] In addition, SMC calculations use incoming plane waves, instead of angular momentum waves, for the homogeneous solution S.

$$S_n = \Phi_n(1 \ldots N) exp(i\mathbf{k}_n \cdot \mathbf{r}_{N+1})$$

Thus this is the only method described in this book which uses a linear momentum instead of an angular momentum representation for the T-matrix. A plane wave representation is chosen because the two-electron integral between three Gaussian functions and one plane wave can be evaluated analytically.[13]

Below, we describe the overall organization of an SMC code, the steps for calculating a body-frame fixed-nuclei T-matrix, T_{mn}, the transformation from the body-frame to laboratory-frame, and the calculation of differential cross sections (dcs). Some of the important features in implementing the SMC method are described in more detail in subsequent sections.

(a) Angular quadrature for $\mathbf{k}_m$ and $\mathbf{k}_n$. In the linear momentum representation, T_{mn} is a function of both the magnitude and direction of $\mathbf{k}_m$ and $\mathbf{k}_n$, $T_{mn} = T(\mathbf{k}_m, \mathbf{k}_n)$. The total energy determines the magnitude of the wave vector, see Eq. (9). To simulate the random orientation of a molecule in a gas phase collision, SMC calculations for gas phase e-molecule collisions are performed over angular quadratures of $\mathbf{k}_m$ and $\mathbf{k}_n$. Thus, instead of positing an electron beam with a fixed direction colliding with randomly oriented molecules, we fix a molecule in space and describe its collision with electrons coming from different directions, (θ, φ). Note that molecular symmetry can be employed to reduce the number of quadrature points used. For example, the cylindrical symmetry of a diatomic molecule allows us to to calculate the plane wave contribution from one φ and deduce the contributions from other φ's by rotation. Also, part (f) shows that the number of partial waves retrieved in a partial wave decomposition of $T(\mathbf{k}_m, \mathbf{k}_n)$ depends on the size of quadrature used.

(b) Gaussian basis set. Gaussian basis sets for the calculation of molecular wave functions have been well studied. A variety of basis sets are available, with varying degree of accuracy.[33] All SMC calculations carried out have used bases constructed with the segmented contraction scheme, including Dunning's earlier contracted basis[34] and his correlated consistent contracted basis.[35] For diatomic molecules and polyatomic hydrides, uncontracted bases have also been used. The Gaussian basis for the continuum electron is obtained by augmenting the target basis with even-tempered diffuse functions. Their exponents are determined by

$$\zeta_{i+1}^{\Gamma} = \frac{\zeta_i^{\Gamma}}{\alpha^{\Gamma}}$$

where ζ_i^{Γ} is the exponent of the i*th* Gaussian of symmetry type Γ and α^{Γ} is a constant, usually between 2 to 3. The initial ζ_i^{Γ} is taken from the most diffuse function of this symmetry type in the target basis. Note that as more diffuse functions are introduced, the basis set is closer to redundancy. Hence, instead of placing diffuse functions at each nuclear center, it becomes advisable to place the most diffuse functions only at the center of mass. Also, if a basis set is truly redundant, the lowest eigenvalue of its overlap matrix is zero. This feature can be used as a quick test for basis set redundancy.

When the Green's function matrix elements are calculated using the insertion technique, an additional basis is needed for the insertion calculation, The choice of this basis, which is critical to the success of the insertion method, will be discussed in Sec. 3.5.

(c) Open and Closed channel functions. The open channel projection operator P is defined to span all energetically accessible target functions. However, in practical calculations it is frequently not feasible to include all open channels defined in this manner, since the size of the calculation will become too large. This problem occurs when the electron energy is close to or larger than the first ionization potential of the target and the full set of Rydberg states, the ionization continuum, and dissociative states become open. Thus a selection process must be made. Generally, a multichannel study is undertaken because a particular set of elastic/excitation processes is of interest. The open channel space should include the initial and final channels for these processes, as well as other open channels which have significant couplings with the channels under study. For example, in a study of valence excitations, Rydberg states are generally neglected because the Rydberg-valence coupling tends to be small.[36] A significant amount of experimentation is required in the selection.

The full Gaussian basis is used to span the continuum electron orbital. This guarantees that the open channel function is invariant when we transform the orbitals to achieve an optimal representation of the closed channel space. Notice that, in the SMC method, terms of the type given in Eqs. (23) and (24), so called penetration terms, belong to the open channel space because they are associated with the open channel target functions and the projection operator P does not annihilate them. In the Kohn method, which employs the Feshbach projector formalism to partition the open and closed channel space, these terms are grouped into the closed channel space instead.

The closed channel functions are chosen so they can describe, in as compact an expansion as possible, the effects of energetically inaccessible channels and/or transient negative ions on the scattering process. For a nonresonant process, the closed channel space contributes to the description of the mutual polarization effects between the target and electron. In the type of trial function used in Eq. (40), this contribution is represented by the use of 1-hole-2-particle configurations obtained by multiplying the dipole-allowed, singly-excited configurations generated from the target function with the continuum orbital. The description "dipole allowed" means the transition dipole moment between the singly excited N-electron CSF and the target function does not vanish. The polarization effect will be accounted for if a complete set of such configurations is included in the trial function.

In practice, however, this will make the calculation quite large, especially if a large one-electron basis is used. Thus truncation of the CSF expansion is necessary. This is achieved by employing natural orbitals derived from bound state calculations. Earlier SMC calculations[37] used natural orbitals from bound state negative ion CI calculations. Because these are bound state calculations, the continuum electron is simulated by a high-lying Rydberg orbital. Nevertheless, the natural orbitals from the CI calculations can be used to provide a shorter expansion for the closed channel functions. A more efficient expansion has recently been proposed by Lengsfield et al.[38] using polarized orbitals, an approach adopted in recent SMC calculations.[22]

For processes involving shape resonances, natural orbitals deduced from a bound state $N + 1$-electron CI still provides an optimal representation of the closed channel space. In the cases we have studied so far, the CI wave function suitable for representing the transient negative ion can be readily identified by the presence, in the set of natural orbitals for this state, of an orbital with an occupation number of nearly one and with a strong antibonding valence character. Based on the size of the corresponding CI coefficients, a truncated CSF list can be generated and then used to generate the closed channel configurations. This approach has been employed to obtain an ac-

curate description of the $^2\Pi_g$ resonance in the elastic scattering of N_2,[39] and the shape resonances in the Be atom and small Be clusters.[22]

Polarization effects are also important for resonant channels so one should generally use a combination of the above two strategies. One can either generate a set of polarized orbitals from the natural orbitals excluded from the description of the transient negative ion, or order the set of discarded CSF's by the transition dipole moment between the N-electron function associated with the CSF and the target state. A recent calculation on elastic scattering of CF_4, incorporating polarization effects, is based on the second approach. Some of the results are presented at the end of part (f).

The SMC method can also be used to study Feshbach resonances which arise from the interaction of the open channel with a bound negative ion associated with an excited target state. The closed channel configurations used to represent a Feshbach resonance can be generated readily using the bound state CI techniques described above. An SMC study of a Feshbach resonance in e-H_2 collisions has been reported.[40] However, this calculation used a frozen core approximation for the excited state orbitals instead of CI natural orbitals.

(d) Integrals. Three type of integrals are involved: (1) The matrix elements $\langle\Psi_m^{(-)}|\hat{H}|\Psi_n^{(+)}\rangle$ and $\langle\Psi_m^{(-)}|V|\Psi_n^{(+)}\rangle$. These matrix elements involve integrals between Gaussians which are evaluated using existing quantum chemistry packages. (2) The matrix elements $\langle\Psi_m^{(-)}|V|S_n\rangle$ and $\langle S_m|V|\Psi_n^{(+)}\rangle$. If V is the nuclear attraction potential, it involves integrals between a Gaussian and a plane wave. If V is the two-electron repulsion potential, the integrals are between three Gaussians and a plane wave. Analytical expressions for both one and two-electron integrals have been derived.[13, 42] These integrals are complex and their evaluation are more costly than the Gaussian integrals. For example, the two-electron integrals are an order of magnitude slower than the corresponding Gaussian integrals. Nevertheless, integral packages are available for their calculation. Note that these integrals are calculated over the angular quadrature of $\mathbf{k}_m, \mathbf{k}_n$. (3) The Green's function matrix element. This type of integrals is considered to be the bottleneck in a Schwinger calculation. They will be discussed separately in Sec. 3.5.

(e) Formation of the $A^{(+)}$ matrix and its inversion. Once the integrals are calculated and the open and closed channel configurations are chosen, the gathering of the $A^{(+)}$ matrix elements follows the structure of quantum chemistry codes. The operation of the projection operator P is also straightforward. For SCF target functions, this operation is done directly but for CI target functions, it can be more efficiently performed using density matrices. In Sec. 3.6 we shall consider how SMC calculations avoid a certain type of pseudoresonance when correlated target functions are used.

Due to the use of complex boundary conditions, the $A^{(+)}$ matrix elements are complex. Its inversion is done using matrix inversion routines for complex matrices available in many computational science libraries. The body-frame $T(\mathbf{k}_m, \mathbf{k}_n)$ is then obtained from Eq. (34) using the inverted $A^{(+)}$ matrix, If the projection parameter a is to be determined variationally, then an iterative solution of a is coupled with the calculation of $T(\mathbf{k}_m, \mathbf{k}_n)$ at this step.

(f) Frame transformation and cross section expression. To obtain the differential cross section, we need to transform the body-frame T-matrix into the laboratory-frame. Let (θ_n, φ_n) and (θ_m, φ_m) be the angular coordinates of $\mathbf{k}_n$ and $\mathbf{k}_m$ in the body-fixed frame. We first expand $T(\mathbf{k}_m, \mathbf{k}_n)$ in terms of partial waves of $(\theta_m,$

$\varphi_m)$

$$T(\mathbf{k}_m, \mathbf{k}_n) = \sum_{l,\mu} T_{l\mu}(k_m, k_n, \varphi_n, \theta_n) Y_{l\mu}(\theta_m, \varphi_m). \tag{41}$$

The body-frame partial wave T-matrix is determined by

$$T_{l\mu}(k_m, k_n, \varphi_n, \theta_n) = \int_o^\pi d\theta_m sin\theta_m \int_o^{2\pi} d\varphi_m Y^*_{l\mu}(\theta_m, \varphi_m) T(\mathbf{k}_m, \mathbf{k}_n).$$

Next the body-frame partial wave T-matrix is transformed to a laboratory-frame with the new Z-axis in the direction of $\mathbf{k}_n$. The Euler angles for the frame transformation is $(0, \theta_n, \varphi_n)$.

$$T^L(\theta, \varphi, \theta_n, \varphi_n) = \sum_{l,\mu,\nu} T_{l\mu}(k_m, k_n, \varphi_n, \theta_n) Y_{l\mu}(\theta_m, \varphi_m) D^l_{\mu\nu}(0, \theta_n, \varphi_n).$$

Here (θ, φ) is the solid scattering angle in the laboratory frame. Then $|T^L|^2$ is averaged over θ_n, φ_n to account for the random orientation of the target,

$$\sigma(\theta, \phi) = \frac{1}{16\pi^3} \frac{k_m}{k_n} \int_o^\pi d\theta_n sin\theta_n \int_o^{2\pi} d\varphi_n |T^L(\theta, \varphi, \varphi_n, \theta_n)|^2.$$

The physical cross section is obtained by averaging over the azimuthal angle φ,

$$\sigma(\theta) = \frac{1}{2\pi} \int_o^{2\pi} d\varphi \sigma(\theta, \varphi).$$

Integration of $\sigma(\theta)$ over θ gives the integral cross section. The integral cross section can also be obtained directly in the body-frame,

$$\sigma = \frac{1}{16\pi^3} \frac{k_m}{k_n} \int d\hat{\mathbf{k}}_n \int d\hat{\mathbf{k}}_m |T(\mathbf{k}_m, \mathbf{k}_n)|^2.$$

It should be mentioned that the number of partial waves deducible from Eq. (41) is determined by the size of the angular quadrature used to calculate the body-frame T-matrix for various plane wave orientations. While in principle each plane wave can be decomposed into an infinite sum of angular momentum waves, the finite angular quadrature used in the calculation limits the number of angular momentum waves obtainable from such decomposition. However, as discussed in part (g), the scattering of high l partial waves can be described by perturbation theory and does not require a full scale variational calculation. Thus the limited number of partial waves deduced from Eq. (41) does not present a problem. In most cases, a (8x8) or (10x10) Gaussian-Legendre quadrature for $\hat{k}_m$ and $\hat{k}_n$ give $l_{max} = 6$ for the angular momentum wave.

A recent calculation of e-CF_4 elastic scattering,[43] including polarization effects, serves as an example of an SMC calculation which employs a set of optimized closed channel configurations. An elastic scattering calculation in the static-exchange (SE) approximation has been reported by Winstead et al.[44] who improved an earlier SE calculation by Huo[45] by employing a larger Gaussian basis. They reported an A_1 resonance at $\approx$ 13 eV and a T_2 resonance at $\approx$ 11 eV. The present polarization calculation used a Gaussian basis of 10s6p1d functions at each nuclear center. The target function was described by an SCF function at the experimental equilibrium geometry and an (8x8) angular quadrature for the wave vector was used. The closed channel space was chosen using the procedure described in part (c) above. Thus bound state CI calculations were carried out for negative ions of $^2A_1$, $^2T_{2x}$, $^2T_{2y}$ and $^2T_{2z}$ symmetries and the CI wave

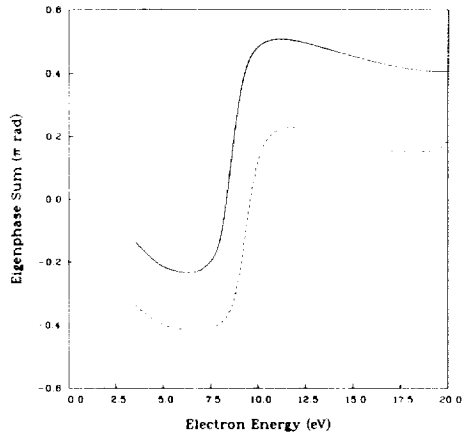

Figure 1. Eigenphase sums for electron-CF_4 scattering, showing resonances in the $^2A_1$ (dashed line) and $^2T_{2x}$ (solid line) partial channels.

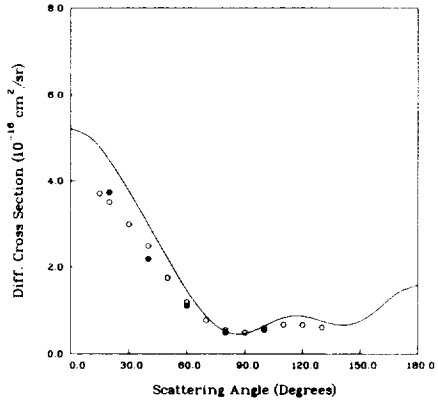

Figure 2. Differential cross section for elastic electron-CF_4 scattering at 8 eV. Solid line, present polarized result, filled circles, experiment of Mann and Linder,[46] and open circles, experiment of Boesten et al.[47]

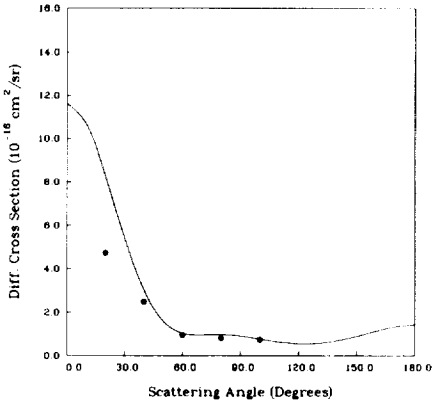

Figure 3. Differential cross section for elastic electron-CF_4 scattering at 11 eV. Solid line, present polarized result, and filled circles, experiment of Mann and Linder.[46]

functions with a strong antibonding character were identified as good candidates to describe the transient negative ions. It was found that the natural orbitals from the $^2A_1$ ion calculation could also provide rather compact representations of the CI functions of the $^2T_{2x}$, $^2T_{2y}$ and $^2T_{2z}$ ions. Thus the $^2A_1$ natural orbitals were used in the scattering calculation and lists of CSF's for the four symmetries were generated from the respective negative ion CI calculations. The lists were augmented to include polarization effects based on the size of the transition moment. They were then used to represent the closed channel functions in the polarized scattering calculation. Figure 1 presents the eigenphase sum of the A_1 and T_{2x} partial channels. The position of the A_1 resonance is lowered to 9.0 eV and the T_2 resonance to 8.6 eV, in much better agreement with experimentally observed features.[46, 47] Figures 2 and 3 present the theoretical differential cross section (dcs) at 8 and 11 eV, together with experimental data.

(g) Born closure for long range potentials. When the interaction potential or transition potential includes long range multiple potentials, such as the dipole potential in elastic scattering or the dipole transition potential in dipole-allowed transitions, the number of partial waves required to converge the cross section, especially in the forward direction, is significantly larger than what can be provided by an SMC calculation with moderate size angular quadrature. On the other hand, due to the large centrifugal barrier for the higher partial waves, they are prevented from reaching the inner region of the target and the scattering tends to be weaker. Thus the Born approximation is expected to be valid for the high l partial waves and can be employed to describe their contributions[48-50] to the cross section. Gibson et al.[41] made use of the following Born closure approximation,

$$\sigma(\theta) = \sigma^{FBA}(\theta) + [\sigma^{SMC}(\theta) - \sigma^{FBA}_{FE}(\theta)]. \tag{42}$$

to include the high l contributions in the dcs. Here FBA denotes the first Born approximation and $\sigma^{FBA}_{FE}(\theta)$ is obtained from a finite expansion of the first Born cross section containing exactly the same number of partial waves as $\sigma^{SMC}(\theta)$. In Eq. (42), the Born value for the low l contributions to the dcs is subtracted out. Thus we use the SMC result for the low l and Born value for the high l contributions to the dcs. In evaluating $\sigma^{FBA}_{FE}(\theta)$, care should be taken so that the same angular quadrature of $\mathbf{k}_m$ and $\mathbf{k}_n$ are used as in the SMC calculation.

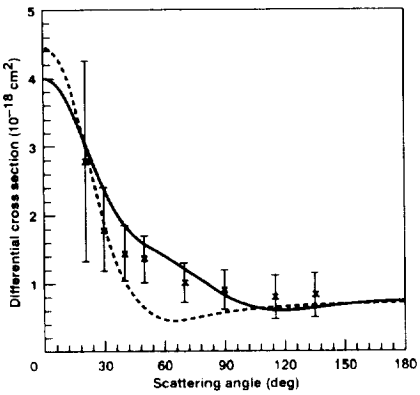

Figure 4. Differential cross section for $X^1\Sigma_g^+ \rightarrow B^1\Sigma_u^+$ transition of H_2 at 15 eV. Solid line, SMC result, dashed line, distorted wave result,[48] and crosses, experimental data of Srivastava and Jensen.[49]

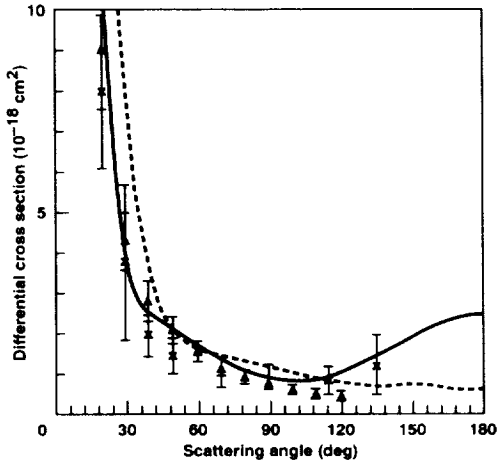

Figure 5. Differential cross section for $X^1\Sigma_g^+ \rightarrow B^1\Sigma_u^+$ transition of H_2 at 20 eV. Solid line, SMC result, dashed line, distorted wave result,[48] crosses, experimental data of Srivastava and Jensen,[49] and triangles, experimental data of Khakoo and Trajmar.[50]

Equation (42) has been applied to a two-channel SMC calculation to study the dipole allowed transition $X^1\Sigma_g^+ \rightarrow B^1\Sigma_u^+$ in H_2. Figures 4 and 5 present the 15 and 20 eV dcs from the SMC calculation with Born closure, the distorted wave calculation of Rescigno et al.,[51] and the experimental data of Srivastava and Jensen[52] and Khakoo and Trajmar.[53]

It should be pointed out that in their implementation of the Born closure approximation to study elastic scattering of polar molecules, Rescigno et al. [4, 54] took a slightly different approach and applied it to the body-frame T-matrix instead of the dcs.

3.5. Evaluation of the Green's Function Matrix Elements

The Green's function matrix element

$$M = \langle \Psi_m^{(-)} | V G_P^{(+)} V | \Psi_n^{(+)} \rangle,$$

can be expressed as

$$M = M_R + iM_I.$$

The imaginary part M_I is given by the residue,

$$M_I = -\frac{i}{8\pi^2} \sum_l k_l \int d\hat{\mathbf{k}}_l \langle \Psi_m^{(-)} | V | S_l \rangle \langle S_l | V | \Psi_n^{(+)} \rangle. \tag{43}$$

where l sums over the poles of $G_P^{(+)}$. Since $G_P^{(+)}$ is a projected Green's function, this is equivalent to a sum over the open channels and k_l is just the wave vector associated with the open channel l. Also, $\langle S_l | V | \Psi_n^{(+)} \rangle$ is the same matrix element used in the expression of the body-frame T-matrix, T_{ln}. The integration over $\hat{\mathbf{k}}_l$ in Eq. (43) can use the same quadrature as the body-frame T-matrix. Consequently, the calculation of M_I involves very little extra work.

The real part of M is given by the principal-value integral,

$$M_R = \frac{1}{(2\pi)^3} \mathcal{P} \int_o^\infty d\epsilon \sum_{l \in open} \frac{k\, U_{mn}}{(E - \mathcal{E}_l) - \epsilon + i\delta}. \tag{44}$$

with

$$U_{mn}(k) = \int d\hat{\mathbf{k}} \langle \Psi_m^{(-)} | V | \Phi_l e^{i\mathbf{k}\cdot\mathbf{r}_{N+1}} \rangle \langle e^{i\mathbf{k}\cdot\mathbf{r}_{N+1}} \Phi_l | V | \Psi_n^{(+)} \rangle, \tag{45}$$

Here $\epsilon = \frac{1}{2}k^2$. Due to the integration over ϵ and $\hat{\mathbf{k}}$, M_R is much more difficult to compute. Its efficient and accurate calculation is an important factor in the development of a practical SMC method. Two approaches to computing this integral are described below.

(a) Direct numerical calculation over a quadrature of $\hat{\mathbf{k}}$ and ϵ. An optimized quadrature is obviously important in this approach. To avoid the rapid variation of the integrand in the ϵ coordinate near the poles of the Green's function, we follow the work of Walters[55] and Heller and Reinhardt[56] and separate the ϵ-integration into two regions, with the poles of the Green's function all located in the first region. The rapid variation in the first integrand is avoided by the addition and subtraction of a term such that the numerical integration can be carried out over a smooth integrand. The ϵ-integral in the first region is rewritten as,

$$I_1 = \sum_{l \in open} \mathcal{P} \int_o^{\epsilon_a} d\epsilon \frac{k\, U_{mn}(k)}{E - \mathcal{E}_l - \epsilon} = \sum_{l \in open} \mathcal{P} \int_o^{\epsilon_a} d\epsilon \left\{ \frac{k\, U_{mn}(k)}{E - \mathcal{E}_l - \epsilon} - \frac{k_l\, U_{mn}(k_l)}{E - \mathcal{E}_l - \epsilon} + \frac{k_l\, U_{mn}(k_l)}{E - \mathcal{E}_l - \epsilon} \right\}, \tag{46}$$

with $\epsilon_a > (E - \mathcal{E}_l)$ for all l. In Eq. (46), the second and third term in the integrand are obtained from the first by replacing $\hat{k}$ and k with $\hat{k}_l$ and k_l. Because $U_{mn}(k_l)$ and k_l are independent of ϵ, the last integral on the right-hand side of Eq. (46) can be evaluated analytically and Eq. (46) is rewritten as,

$$I_1 = \sum_{l \in open} \left\{ k_l\, U_{mn}(k_l)\, ln\left(\frac{\epsilon_l}{\epsilon_a - \epsilon_l} \right) + \mathcal{P} \int_o^{\epsilon_a} d\epsilon \left[\frac{k\, U_{mn}(k)}{E - \mathcal{E}_l - \epsilon} - \frac{k_l\, U_{mn}(k_l)}{E - \mathcal{E}_l - \epsilon} \right] \right\}.$$

Since the first and second term in the ϵ-integand above have poles at the same place, the large changes in the integrand near the pole region are canceled out and the integrand remains smooth, suitable for numerical integration.

To demonstrate the convergence of the numerical quadrature scheme, we calculated the elastic scattering of CO in the static-exchange approximation, using an SCF target at the experimental equilibrium geometry. A Gaussian basis, with 5s3p1d contracted functions at each nuclear center, represented the continuum electron. The SMC calculation included up to $l_{max} = 6$. Born closure was not included since our purpose was to demonstrate the convergence of the $VG_P^{(+)}V$ quadrature, and the introduction of a constant correction term from the Born closure would not affect our conclusions. Also, all calculations used the Gauss-Legendre quadrature.

Figure 6 presents the partial integral cross section for e-CO elastic scattering. A (20x20) quadrature was used for the angular integration and a 20-point quadrature for the second region ϵ integral. Three different quadratures were used for the first ϵ region, 20, 32, and 48 points. The three cross section curves virtually coalesce, indicating a well converged result.

The cross section is much more sensitive to the quadrature used in the second ϵ integration. Figure 7 shows the cross sections obtained using 20, 32, and 48 quadrature points for the second region integration and keeping the other quadratures constant. Note that the peak of the cross section curve at $\approx$ 3.5 eV, arising from the $^2\Pi$ shape resonance in CO, is shifted to a lower energy when a larger quadrature is used. Also, the 32- and 48-point calculations have similar resonance positions, but the cross sections themselves differ by $\approx$ 10% at the peak.

Sensitivity to the angular quadrature was also studied. Figure 8 presents the results for the variation in the θ quadrature, keeping all other integration parameters constant. While the 32- and 48-point integrations give substantially similar results, the 20-point quadrature has not yet converged. In particular, note that the maximum of the cross section, at $\approx$ 3.5 eV energy, is shifted to a higher energy when a larger quadrature is used.

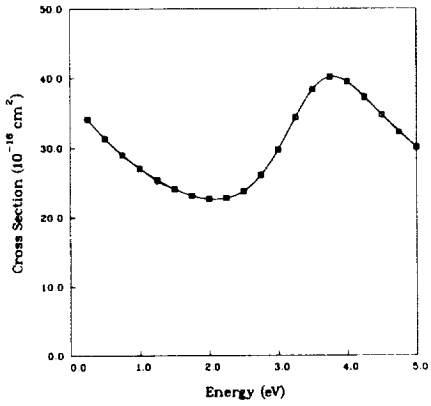

Figure 6. Partial integral cross section (l_{max}=6) for e-CO elastic scattering in the static-exchange approximation. A (20x20) quadrature is used for the angular integration in the $VG_P^{(+)}$V term and 20-point for the second region ϵ-integration. The quadrature size for the first region ϵ-integration is: circle, 20 points, square, 32 points, and triangle, 48 points.

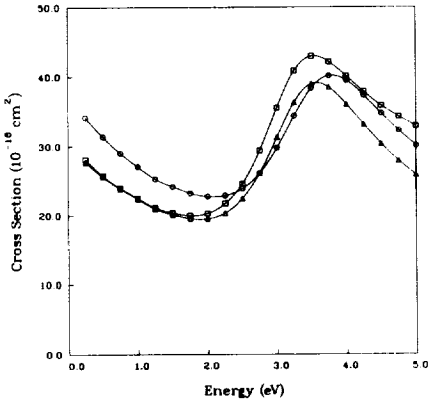

Figure 7. Same as Fig. 6. A (20x20) quadrature is used for the angular integration and 20-point for the first region ϵ-integration. The quadrature size for the second region ϵ-integration is: circle, 20 points, square, 32 points, and triangle, 48 points.

When a bigger basis set is used for the target function, the demand for a larger angular quadrature becomes higher, particularly if the basis set is uncontracted and has very large exponents. Also, the second ϵ integral shows more sensitivity to the size of the angular quadrature. These features suggest that the off-shell contribution to the $VG_P^{(+)}V$ term, coming from the high energy region of the target spectrum, may be responsible for the need of large quadratures. In the above example, a converged result requires over forty thousand quadrature points.

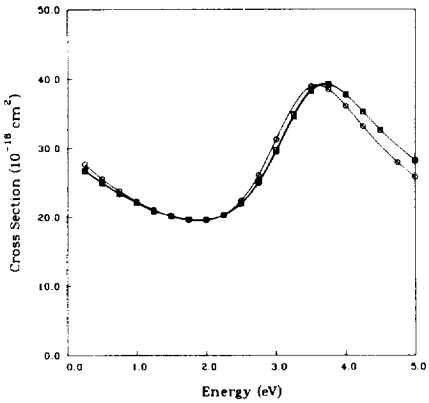

Figure 8. Same as Fig.6. A 20-point quadrature is used for the first region ϵ-integration, 48 for the second, and 20 for the φ integration. Circle, 20-point θ quadrature, square, 32 points, and triangle, 48 points.

The direct numerical integration approach was first investigated by Lima et al.[57] To expedite the integral calculation, Winstead et al.[58] have successfully adapted the integral calculation and the three-index transformation[5/] to the highly parallel computers. Parallel computers are particularly well suited for this purpose because each integral calculation is independent of others. SMC calculations using this technique have been carried out on many polyatomic molecules.[12]

(b) Insertion using a Gaussian basis. Provided that a Gaussian basis satisfies the approximate relation

$$\sum_a |p_a\rangle\langle p_a| \approx 1.$$

the free-particle Green's function can be projected into this basis, called the insertion basis. The principal-value Green's function matrix element is now written as

$$M_R = \frac{1}{(2\pi)^3} \sum_{l\in open} \sum_a \sum_b \langle \Psi_m^{(-)}|V|\Phi_l\, p_a(\mathbf{r}_{N+1})\rangle\langle \Phi_l\, p_b(\mathbf{r}_{N+1})|V|\Psi_n^{(+)}\rangle$$

$$\times \mathcal{P}\int_o^\infty d\epsilon \int d\hat{\mathbf{k}}\, k\, \frac{\langle p_a(\mathbf{r}_{N+1})|e^{i\mathbf{k}\cdot\mathbf{r}_{N+1}}\rangle\langle e^{i\mathbf{k}\cdot\mathbf{r}_{N+1}}|p_b(\mathbf{r}_{N+1})\rangle}{(E-\mathcal{E}_l)-\epsilon+i\delta}. \qquad (47)$$

Both ϵ and $\hat{\mathbf{k}}$ integrals are expressed in closed form.[59] Furthermore, calculations of these Gaussian integrals are an order of magnitude faster than the three-Gaussian-one-plane wave integrals in Eq. (45).

It is important to recognize that in Eq. (47), an L^2 basis is used in the evaluation of an integral over the Green's function, but not to represent the Green's function itself. Just as an L^2 basis can be used to represent a trial function in a Schwinger variational calculation because the trial function is always multiplied by V in the expression of the T-matrix, in the present case the free-particle Green's function is integrated over $V|\Psi^{(+)}\rangle$, with the trial $\Psi^{(+)}$ itself expressed in terms of another L^2 basis. Thus, the *long range oscillatory* part of the Green's function does not contribute to the integral. In this respect, the application of an L^2 basis to evaluate M_R is analogous in spirit to

[5/] The fourth index is the plane wave.

Schneider's calculation[60] of the Schwinger separable potential by projection onto an L^2 basis.

The insertion technique was used in early SMC calculations when large, uncontracted Gaussian bases were used for the scattering basis, with the insertion basis usually composed of the scattering basis supplemented by additional Gaussians. Good convergence behavior was observed.[39] The change to the direct numerical integration technique by Lima et al.[57] was motivated by the convergence problems they encountered. Such problems appeared to be related to choosing a suitable insertion basis.

In view of recent progress made in the field of quantum chemistry in developing flexible Gaussian bases,[33] and the efficiency in the computation of Gaussian integrals themselves, we re-investigated the insertion technique.[20] The choice of a suitable basis was guided by the convergence characteristics observed in the numerical integration approach, namely that the off-shell high energy contribution to M_R seems to play an important role in the convergence. To describe this type of contribution, we included Gaussians with large exponents. Also, a multicentered Gaussian basis readily simulates the dependence on the angular quadrature. When the insertion basis was chosen using these guidelines, good convergence was observed. As an example, we studied the e-CO static-exchange problem using the same scattering basis as discussed above. The insertion basis is obtained by supplementing the scattering basis by 10s18p9d Gaussians at each nuclear center and 16s5p9d Gaussians at the center of mass.[6/] Figure 9 compares the cross sections obtained using the insertion method versus the direct numerical integration approach. Good agreement is observed. The largest discrepancy between the two results, less than 3%, is found at the low energy region. In the $^2\Pi$ shape resonance region, the two curves almost coalesce.

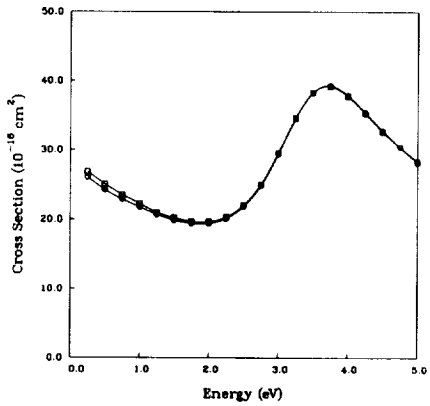

Figure 9. Partial integral cross section (l_{max}=6) for e-CO elastic scattering in the static-exchange approximation. Square, calculated using a direct numerical integration, and circle, calculated with the insertion technique. The numerical integration uses a (32x32) angular quadrature, 20-point for the first ϵ integration, and 48-point for the second. The insertion basis is described in the text.

While the insertion basis used for the CO calculation appears to be very large, it should be pointed out that the insertion basis has 238 Gaussian functions and the total number of Gaussian integrals used is 15.2 million. The numerical integration calculation

[6/] Not all components of the d functions were used. Also, a smaller size p_z basis was used at the nuclear center.

requires more than 2.78 billion three-Gaussian-one-plane wave type integrals.[7/] Taking into account the difference in the cycle time required to calculate the two types of integrals, the insertion technique requires orders of magnitude less CPU and storage resources.

Recently, Bettega et al.[61] applied the pseudopotential method and removed the core electrons from the SMC calculations. This raises an interesting question. Since the off-shell high energy contribution to M_R that we observed originate, at least partially, from the core electrons, the use of pseudopotentials may lessen the demand for large quadratures in the numerical integration technique and the demand for tight Gaussians in the insertion technique. This aspect remains to be tested.

3.6. Correlated Target Function in the SMC Method

Because molecular bonding changes with nuclear geometry, multiconfiguration wave functions are required to provide a consistent description of the target over a range of geometries. Similarly, the description of several electronic states with a common set of orbitals, a practice frequently used in the study of electronic excitations by electron or photon impact, requires the use of multiconfiguration target functions. Thus correlated target functions are used with some frequency in *ab initio* studies of e-molecule collisions.[62-65]

An ubiquitous feature in the use of multiconfiguration target functions is the presence of pseudoresonances at intermediate energies.[62, 65] Lengsfield and Rescigno[62] attributed these resonances to the fact that multiconfiguration target functions can introduce certain terms in the $N+1$-electron wave function which are associated with excited states of the target excluded from the open channel space. Pseudoresonances appear at an energy where the excited target state becomes open. Consider the example of a two-configuration function for the ground state of H_2[8/]

$$\Phi_X = a_1\phi_1 + a_2\phi_2,$$

with

$$\phi_1 = \mathcal{A}\{1\sigma_g\alpha(1)1\sigma_g\beta(2)\},$$
$$\phi_2 = \mathcal{A}\{1\sigma_u\alpha(1)1\sigma_u\beta(2)\}.$$

Here Φ_X is the simplest function that can describe the dissociation of H_2 properly.

Two $N+1$-electron CSF's are used to relax the orthogonality between the target and the continuum electron,

$$\Theta_a = \mathcal{A}_{N+1}\Big\{\Phi_X(1,2)1\sigma_g\alpha(3)\Big\} = a_2\mathcal{A}_{N+1}\Big\{\phi_2(1,2)1\sigma_g\alpha(3)\Big\}.$$

and

$$\Theta_b = \mathcal{A}_{N+1}\Big\{\Phi_X(1,2)1\sigma_u\alpha(3)\Big\} = a_1\mathcal{A}_{N+1}\Big\{\phi_1(1,2)1\sigma_u\alpha(3)\Big\}.$$

Here $\mathcal{A}_{N+1}$ antisymmetrizes electron 3 with electrons 1 and 2. Note that Θ_a includes the terms $1\sigma_g\alpha(1)1\sigma_u\alpha(2)1\sigma_u\beta(3)$ and $1\sigma_g\alpha(1)1\sigma_u\beta(2)1\sigma_u\alpha(3)$. These terms are associated with the $b^3\Sigma_u^+$ target state, with the $1\sigma_u$ orbital representing the continuum electron. In the Kohn calculation it was found that if the $b^3\Sigma_u^+$ state was not included in the open

[7/] As a result of symmetry operations, in both cases the actual number of distinct integrals to be calculated are less. However, the ratio of the the two numbers will be approximately the same when symmetry is taken into account.

[8/] This example was originally used by Lengsfield and Rescigno.[4, 62]

channel space, a pseudoresonance would occur around the energy where this channel became open. Similar pseudoresonances were also observed in the R-matrix calculation of the electronic excitations of H_2.[65] The strategy used in the Kohn method to eliminate such terms has been discussed.[4, 62]

Due to the use of the N-electron projection operator, the SMC method treats correlated target functions differently. As seen in Sec. 3.1, the N-electron projection operator selects the terms that are associated with the target function from an antisymmetrized $N + 1$-electron CSF, resulting in an un-antisymmetrized product of the N-electron target function and an one-electron orbital describing the continuum electron. For a multiconfiguration target function, this operation has additional consequences. As an illustration, consider the same two-configuration wave function. The projection operator P is given by

$$P = |\Phi_X\rangle\langle\Phi_X|.$$

The operation of P on Θ_a gives,

$$P|\Theta_a\rangle = \frac{a_2}{\sqrt{3}}\Phi_X(1,2)1\sigma_g\alpha(3).$$

Thus the operation of P recovers the ϕ_1 component in Θ_a, originally eliminated by antisymmetrization. In this manner, the projector P removes the $b^3\Sigma_u^+$ character from Θ_a, and $P\Theta_a$, unlike Θ_a itself, consists only of the open channel target.

In an SMC calculation, a pseudoresonance usually appears when the denominator in the expression of the T-matrix becomes particularly small at a certain energy. Because Θ_a includes a term that behaves like a open channel function, the matrix element

$$\langle\Psi^{(-)}|\hat{H}|\Theta_a\rangle,$$

as a function of energy E goes through a minimum around the energy when that channel becomes open. On the other hand, $P\Theta_a$ does not have any $b^3\Sigma_u^+$ character, and

$$\langle\Psi^{(-)}|\hat{H}P|\Theta_a\rangle,$$

does not exhibit the same minimum.

Based on this analysis, an SMC calculation is expected to perform differently from other methods when a multiconfiguration target is used. Figure 10 presents an SMC study of the $^2\Sigma_g^+$ channel elastic scattering of H_2, using the static-exchange approximation. The calculation was carried out at $R = 4.0\ a_o$, using a Gaussian basis of 6s6p at H and 4s4p at the center of mass, The CI coefficients of the two-configuration target function are 0.8785 and -0.4778. As seen in Fig. 10, the SMC cross section curve is smooth over the energy range of 0.25 to 21 eV. The pseudoresonance found in other methods, arising due to the term Θ_a, is absent here. Thus it appears that the role of the projection of P on Θ_a is to associate Θ_a with the correct open channel, and thereby removes the spurious resonance.

The above results suggests that the N-electron projection operator has additional advantages besides providing a convenient treatment for exchange. The use of correlated target function in the SMC method is relatively recent. Only a few studies have been made using a multiconfiguration target function.[22] Future studies should explore this aspect further.

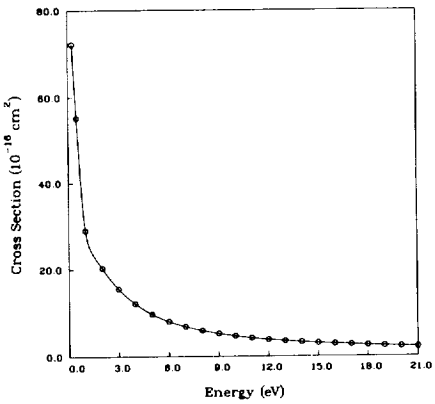

Figure 10. Integral cross section for e-H_2 $^2\Sigma_g^+$ channel elastic scattering in the static-exchange approximation, calculated using a two-term CI function for the target

4. THE USE OF SMC RESULTS IN THE STUDY OF VIBRATIONAL EXCITATIONS

All SMC calculations use the fixed-nuclei approximation. However, the fixed-nuclei SMC results can be readily used as a starting point in the application of the nuclear dynamics treatment of Domcke. Domcke's treatment, which is based on the projection operator formalism, has been reviewed recently,[23] and it will not be repeated. Here we consider an example of combining the two approaches in the study of the resonant enhanced vibrational excitation of N_2 by electron impact. Because the $^2\Pi_g$ resonance in N_2 is a pure d-wave resonance, we rewrite the T-matrix for the l=2 partial wave in terms of the K-matrix,

$$T_{l=2}(E,R) = \frac{K(E,R)}{1 - iK(E,R)} ,$$

where R is the internuclear distance. The K-matrix element is related to the width $\Gamma(E,R)$ and shift $\Delta(E,R)$ functions by

$$K(E,R) = -\frac{\Gamma(E,R)}{2[E - \epsilon_d(R) - \Delta(E,R)]} .$$

Here ϵ_d is the difference between the target and negative ion potential curves. The shift function is given by the principal value integral,

$$\Delta(E,R) = \frac{1}{2\pi}\mathcal{P}\int dE' \frac{\Gamma(E',R)}{E - E'},$$

and the width function can be expressed in terms of the potential U_{dE} which Domcke called the entry amplitude,

$$\Gamma(E,R) = 2\pi|U_{dE}|^2.$$

An analytical fit of U_{dE} can be obtained using the K-matrix determined from the SMC calculation. Notice that U_{dE} is a nonlocal potential, depending on both R and E.

The calculation on N_2 has been reported previously.[39, 66] In applying Domcke's method, we used a Schwinger-type separable potential approach to evaluate the T-matrix element. A complete set of the bound vibrational wave function of the transient

negative ion, obtained using a numerical solution of the 1-d schrödinger equation, was used in the separable potential calculation. The negative ion curve was determined empirically by Berman et al.[67]

The results of this calculation compared well with experiment, and the comparison will not be repeated. Here we consider an example of applying our result to an experimentally inaccessible region. In very high temperature plasmas, as in the flow field of a high-speed space vehicle upon entry to the earth's atmosphere, molecules are very hot ro-vibrationally and it is difficult to duplicate such conditions in the laboratory. Figure 11 presents the $v = 0 \rightarrow 1$ and $v = 3 \rightarrow 4$ vibrational excitation cross sections of N_2 by electron impact. While many experimental measurements on transitions from $v = 0$ have been done, there has been only one reported measurement with the initial state at the $v = 1$ level.[68] Due to the difficulties involved in preparing a significant quantity of N_2 at the $v = 3$ level, no measurement has been reported for excitations from this level and theoretical data is the only available source for these cross sections. It is seen from Fig. 11 that the resonance structures for the $v = 3 \rightarrow 4$ transition is more extended both at high and low energies in comparison with the $v= 0 \rightarrow 1$ transition, and not as strongly peaked. The calculation assumed the molecule was initially at $J = 50$, with the centrifugal barrier in the vibrational potential determined by this J value. Note that our calculation did not include rotation in the dynamics and the effect of rotation only entered through the centrifugal term.

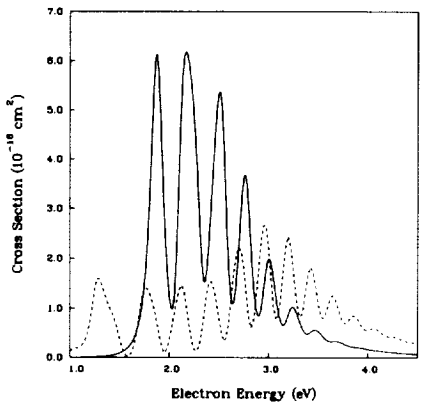

Figure 11. N_2 vibrational excitation cross sections by electron impact. Solid line, $v = 0 \rightarrow 1$, dashed, $v = 3 \rightarrow 4$. The calculation assumes the molecule is at $J = 50$.

Figure 12 presents the $v = 0 \rightarrow 1$ excitation cross sections for N_2 at J=0, 50, and 150. Again rotational effects contribute only through the centrifugal barrier of vibrational motion. Because the differences between the potential curves of the neutral and transient negative ion, the large centrifugal barriers at $J = 50$ and 150 have differential effects on the vibrational excitation. The resonance structure in the cross section moves to lower energies and narrows as J increases.

Future studies that couple vibrational and rotational motion at high J will extend our understanding of the collisional processes involving ro-vibrationally hot molecules.

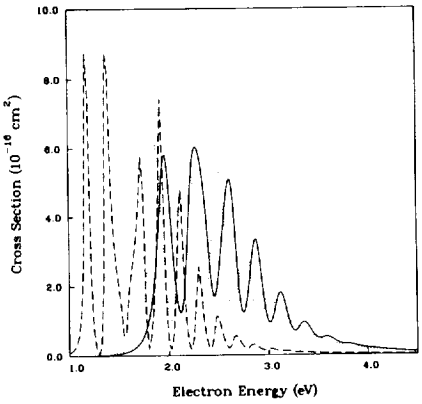

Figure 12. N_2 $v = 0 \rightarrow 1$ vibrational excitation cross section by electron impact. Solid line, $J = 0$, dotted, J=50, and dashed, J= 150.

5. SUMMARY

The SMC method, a modified version of the SV method, has proven to be a versatile tool in the study of e-molecule collisions. The SMC method has been successfully applied to the study of technologically important electron collision processes involving polyatomic targets. This application will continue as the SMC method is further developed and refined. The present discussion of its implementation also serves to illustrate some of the physical basis in its formulation, and provides a foundation for the future development of the method.

References

[1] L. Hulthén, Kgl. Fysiograf. Sälbkap. Lund. Fröh. **14**, 257 (1944).

[2] W. Kohn, Phys. Rev. **74**, 1763 (1948).

[3] S.I. Rubinow, Phys. Rev. **96**, 218 (1954).

[4] T.N. Rescigno, C.W. McCurdy, A.E. Orel, and B.H. Lengsfield III, "The Complex Kohn Variational Method," chapter 1 in this book.

[5] J.L. Jackson, Phys. Rev. **83**, 301 (1951).

[6] R.K. Nesbet, *Variational Methods in Electron-Atom Scattering Theory*, Plenum Press, New York (1980).

[7] B.I. Schneider, "An R-Matrix Approach to Electron Molecule Collisions," chapter 8 in this book.

[8] J. Schwinger, Phys. Rev. **56**, 750 (1947).

[9] R.R. Lucchese, K. Takatsuka, and V. McKoy, Phys. Rep. **131**, 147 (1986).

[10] D.K. Watson, Adv. At. Mol. Phys. **25**, 221 (1988).

[11] M.A.P. Lima, T.L. Gibson, L.M. Brescansin, V. McKoy, and W.M. Huo, "Studies of Elastic and Electronically Inelastic Electron-Molecule Collisions," in *Swarm Studies and Inelastic Electron-Molecule Collisions*, ed. L.C. Pitchford, B.V. McKoy, A. Chutjian, and S. Trajmar, Springer-Verlag, New York (1987), pp 239-264.

[12] C. Winstead and V. McKoy, "Studies of Electron-Molecule Collisions on Highly Parallel Computers," in *Modern Electronic Structure Theory Vol. 2*, ed. D. Yarkony, World Scientific, Singapore (1994).

[13] D.K. Watson and V. McKoy, Phys. Rev. A **20**, 1474 (1979).
[14] R.R. Lucchese, G. Raseev, and V. McKoy, Phys. Rev. A **25**, 2572 (1982).
[15] See, for example, G. Bandarage and R.R. Lucchese, Phys. Rev. A **47**, 1989 (1993); M.-T. Lee, K. Wang, and V. McKoy, J. Chem. Phys. **97**, 3108 (1992).
[16] M.-T. Lee, M.M. Fujimoto. S.E. Michelin, L.E. Machado, and L.M. Brescansin, J. Phys. B. **25**, L505 (1992).
[17] M.-T. Lee, S.E. Michelin, L.M. Brescansin, G.D. Meneses, and L.E. Machado, J. Phys. B. **26**, L477 (1993).
[18] K. Takatsuka and V. McKoy, Phys. Rev. A **24**, 2473 (1981).
[19] K. Takatsuka and V. McKoy, Phys. Rev. A **30**, 1734 (1981).
[20] W.M. Huo and J.A. Sheehy (to be published).
[21] C. Winstead, Q. Sun, and V. McKoy, J. Chem. Phys. **97**, 9483 (1992).
[22] W.M. Huo and J.A. Sheehy, "Theoretical Study of Electron Scattering by Small Clusters and Adsorbates," in *Electron Collisions with Molecules, Clusters, and Surfaces*, ed. H. Ehrhardt and L.A. Morgan, Plenum, New York (1994), pp 171-182.
[23] W. Domcke, Phys. Rep. **208**, 97 (1991).
[24] R.G. Newton, *Scattering Theory of Waves and Particles*, Springer-Verlag, New York (1982).
[25] B.H. Bransden, R. Hewitt, and M. Plummer, J. Phys. B **21**, 2645 (1988).
[26] S.K. Adhikari and I.H. Sloan, Phys. Rev. C **11**, 1133 (1975).
[27] K. Takatsuka, R.R. Lucchese, and V. McKoy, Phys. Rev. A **24**, 1812 (1981).
[28] J.T. Taylor, *Scattering Theory*, R. E. Krieger Publishing, FL (1983), pp. 274-279.
[29] H. Feshbach Ann. Phys. **5**. 357 (1958); *ibid* **19**, 287 (1962).
[30] M.A.P. Lima and V. McKoy, Phys. Rev. A **38**, 501 (1988).
[31] W.M. Huo and C.A. Weatherford, Bull. Am. Phys. Soc. **36**, 1265 (1991).
[32] C. Winstead and V. McKoy, Phys. Rev. A **47**, 1514 (1993).
[33] T. Helgaker and P.R. Taylor, "Gaussian Basis Sets and Molecular Integrals" in *Modern Electronic Structure Theory Vol. 2*, ed. D. Yarkony, World Scientific, Singapore (1994).
[34] T.H. Dunning, J. Chem. Phys. **53**, 2823 (1970).
[35] T.H. Dunning, J. Chem. Phys. **90**, 1007 (1989), and D.E. Woon and T.H. Dunning, J. Chem. Phys. **98**, 1358 (1993).
[36] As an example of valence excitation calculations which neglected Rydberg states in the open channel configurations, see Q. Sun, C. Winstead, V. McKoy, J.S.E. Germano, and M.A.P. Lima, Phys. Rev. A **46**, 2462 (1992).
[37] W.M. Huo, M.A.P. Lima, T.L. Gibson, and V. McKoy, Phys. Rev. A **36**, 1642 (1987).
[38] B.H. Lengsfield, T.N. Rescigno, and C.W. McCurdy, Phys. Rev. A **44**, 4296 (1991).
[39] W.M. Huo, T.L. Gibson, M.A.P. Lima, and V. McKoy, Phys. Rev. A **36**, 1632 (1987).
[40] A.J.R. da Silva, M.A.P. Lima, L.M. Brescansin, and V. McKoy, Phys. Rev. A **41**, 2903 (1991).
[41] T.L. Gibson, M.A.P. Lima, V. McKoy, and W.M. Huo, Phys. Rev. A **35**, 2473 (1987).
[42] N.S. Ostlund, Chem. Phys. Letters, **34**, 419 (1975).
[43] W.M. Huo and J.A. Sheehy (to be published). See also J.A. Sheehy and W.M. Huo, "Low-Energy Elastic Electron Scattering from Carbon Tetrafluoride" in ICPEAC

Abstracts Vol. I, ed. T. Andersen, B. Fastrup, F. Folkmann, H. Knudsen, (1993), p. 259.
[44] C. Winstead, Q. Sun, and V. McKoy, J. Chem. Phys. **98**, 1105 (1993).
[45] W.M.Huo, Phys. Rev. A **38**, 3303 (1988).
[46] A. Mann and F. Linder, J. Phys. B **25**, 545 (1992).
[47] L. Boesten, H. Tanaka, A. Kobayashi, M.A. Dillon, and M. Kimura, J. Phys. B **25**, 1607 (1992).
[48] D.W. Norcross and N.T. Padial, Phys. Rev. A **25**, 226 (1982).
[49] S. Chung and C.C. Lin, Phys. Rev. A **17**, 1874 (1978).
[50] A.W. Fliflet and V. McKoy, Phys. Rev. A **21**, 1863 (1980).
[51] T.N. Rescigno, C.W. McCurdy, Jr., and V. McKoy, J. Phys. B **7**, 2396 (1974).
[52] S.K. Srivastava and S. Jensen, J. Phys. B **10**, 3341 (1977). See S. Trajmar, D.F. Register, and A. Chutjian, Phys. Rep. **97**, 219 (1983) for renormalization of this data.
[53] M.A. Khakoo and S. Trajmar, Phys. Rev A **34**, 146 (1986).
[54] T.N. Rescigno, B.H. Lengsfield, C.W. McCurdy, and S.D. Parker, Phys. Rev. A **45**, 7800 (1992).
[55] H.J.R. Walters, J. Phys. B **4**, 437 (1971).
[56] E.J. Heller and W.P. Reinhardt, Phys. Rev. A **7**, 365 (1973).
[57] M.A.P. Lima, L.M. Brescansin, A.J.R. da Silva, C. Winstead, and V. McKoy, Phys. Rev. A **41**, 327 (1990).
[58] C. Winstead, P.G. Hipes, M.A.P. Lima, and V. McKoy, J. Chem. Phys. **94**, 5455 (1991).
[59] D.A. Levin, A.W. Fliflet, M. Ma, and V. McKoy, J. Comp. Phys. **28**, 416 (1978).
[60] B.I. Schneider, Phys. Rev. A **31**, 2188 (1985).
[61] M.H.F. Bettega, L.G. Ferreira, and M.A.P. Lima, Phys. Rev. A **47** 1111 (1993).
[62] B.H. Lengsfield III and T.N. Rescigno, Phys. Rev. A **44**, 2913 (1991).
[63] T.N. Rescigno, B.H. Lengsfield III, and A.E. Orel, J. Chem. Phys. **99**, 5097 (1993).
[64] C.J. Gillan, O. Nagy, P.G. Burke, L.A. Morgan and C.J. Noble, J. Phys. B **20**, 4585 (1987).
[65] S.E. Branchett and J. Tennyson, Phys. Rev. Letts. **64**, 2889 (1990).
[66] W.M. Huo, V. McKoy, M.A.P. Lima, and T.L. Gibson, "Electron-Nitrogen Molecule Collisions in High-Temperature Nonequilibrium Air," in *Thermalphysical Aspects of Re-entry Flows*, ed. J.N. Moss and C.D. Sott, AIAA, New York (1986), pp. 152-196.
[67] M. Berman,H. Estrada, L.S. Cederbaum, and W. Domcke, Phys. Rev. A**28**, 1363 (1983).
[68] S.F. Wong, J.A. Michejda, and A. Stamatovic, unpublished data.